



Jesse Baker and John Miller

ABSTRACT

Automotive door handle systems continue to enhance user experience, safety, and reliability by incorporating new features and improving upon old ones. These features are enabled by different sensing technologies including magnetic sensors (anisotropic magneto resistive (AMR) and Hall-effect), capacitive sensors, and inductive sensors.

This document demonstrates the implementation of a deployable automotive door handle using magnetic and capacitive sensors to capture position data in a door handle demo design. Sensor design and testing methods are described, leveraging the hardware and software based demo, along with potential error sources and alternative sensing options, such as inductive sensing. The technologies covered in this app note include a Hall-effect sensor for detecting the open or close status of the door and an AMR angle sensor for the position of the handle. The application note illustrates the use and design of capacitive sensing for a touch button and the presence of a user's hand on the handle. This application note, but not the demo, also includes the use, design and implementation of an inductive sensor push button (as opposed to a capacitive touch button), as that is also a frequent option in today's vehicles.

Table of Contents

1 Introduction	2
2 Automotive Door Handle Architectures	2
3 Functional Demo Design	3
4 Detailed Design Flow for Door Handle Functions	6
4.1 Door Open or Closed Detection With Magnetic Sensing.....	6
4.1.1 Demo Implementation of Open Close Detection Using TMAG5131-Q1.....	6
4.2 Deployable Door Handle Position Detection With Magnetic Sensing.....	8
4.2.1 Demo Implementation of Deployable Door Handle Position Sensing Using TMAG6180-Q1.....	9
4.3 Hand Proximity Detection With Capacitive Sensing.....	11
4.3.1 Overview of Capacitive Sensing Applications.....	11
4.3.2 Examples of Soft-Touch Detection Based on Capacitive Sensing in a Door Handle Demo.....	13
4.4 Push Button With Inductive Sensing.....	16
4.4.1 Inductive Push Buttons.....	16
4.4.2 Inductive Push Button Sensitivity.....	18
4.4.3 Target Material.....	18
4.4.4 Target Distance and Sensor Size.....	19
4.4.5 Design Example.....	20
5 Summary	23
6 References	23

Trademarks

All trademarks are the property of their respective owners.

1 Introduction

This document provides a high-level overview of automotive door handles and the potential features, and how such features can be achieved using magnetic, capacitive, and inductive sensors. Design examples presented are based on a demo, which is also featured in the demo video [Designing with position sensors: Automotive door handles](#) and the [Position Sensing in Automotive Door Handle Systems](#) application brief.

The demo is used as a foundation to illustrate the use of Hall-based sensors to monitor door open/closed position, and discusses the design considerations and capabilities of Hall sensing technology for this application. This is supported by simulations in [TI Magnetic Sense Simulator \(TIMSS\)](#), TI's online simulator for magnetic position sensors.

The demo also illustrates capacitive-sensing technology as the basis for a touch button to detect a user's finger or hand, which can subsequently deploy a recessed door handle. Once the handle is deployed, a capacitive sensor can then detect the presence of a user's hand on the handle to prevent the handle closing on the user's hand. Approximate mathematical models are given to provide the user a starting point for a design, and the approximations are confirmed by the demo. References to other capacitive sensing application notes with supporting information are given throughout.

Also included in this application note is the use of inductive sensors for *push-button* applications (as opposed to a capacitive *touch button*). This technology is not included in the demo, but is a popular feature in many of today's vehicles. That section covers design and implementation-related considerations and provides a more detailed design example of a push-button sense coil using the [Inductive Sensing Calculator Tool](#).

2 Automotive Door Handle Architectures

From driver and passenger doors to hood and tailgate release systems, automotive door handles come in several different mechanical form factors. Rotational and parallel deployable door handles are typically flush with the body of the door in their home position. An actuator extends the handle outward to present the handle to the user under desired circumstances. Fixed flush door handles do not move, and instead involve a surface or cavity recessed into the door. Hood and tailgate release systems often make use of a push button or soft touch function to trigger the opening of the door. Each of the aforementioned door handle architectures make use of one or several features from a common set of functions found across different door handle systems, some of which are outlined in the following text.

One critical and common safety feature in any vehicle is detecting when the vehicle doors are either opened or closed. It is imperative for the driver to know if any doors are opened while operating the vehicle, and to have confidence knowing the doors are properly closed when leaving the vehicle.

In deployable door handle systems, reliably tracking the door handle's position as it is extended and retracted provides several benefits. Knowing where the handle is along its arc of travel ensures the door handle is deployed and retracted to the proper positions each time, providing a smooth user experience. This function also prevents damage to the door handle by the actuator over-driving the handle, or can help detect if something is stuck in the handle track. Finally, this feature can even detect when a user is pressing or pulling on the door handle.



Figure 2-1. Deployable Door Handle in Extended Position

Soft-touch or hand proximity detection enables either a gentle press or simply the presence of the driver's hand to trigger different actions within the automotive system. In the case of deployable door handles, this function can serve as an alternative method for triggering the extension of the handle. In fixed flush door handles, the handle is a surface or cavity recessed into the vehicle and does not move. In this case, a soft touch on the handle or a hand in close proximity to the handle can be detected and trigger the opening of the car door.



Figure 2-2. Soft-Touch or Hand Proximity Detection for Deployable Door Handle



Figure 2-3. Recessed Cavity for Fixed-Flush Door Handle

Some automotive doors or door handles integrate the use of a button press, such as a hood touch button, door keypad, push-button, or tailgate release system.

3 Functional Demo Design

The functional prototype shown in [Figure 3-1](#) was built to demonstrate how some of the aforementioned functions are achieved within door handle systems: deployable door handle position detection using the [TMAG6180-Q1](#), door open/closed detection using the [TMAG5131-Q1](#), and hand proximity detection and soft touch detection using the [FDC1004-Q1](#).



Figure 3-1. Front View of Door Handle Demo

The front-view of the demo shows the 3D printed door frame, door and hinges, deployable door handle, power switches, and base plate. The leftmost switch controls the 12V power to the demo. The middle switch interrupts the output from the motor driver going to the motor. The rightmost switch is included for future implementation of interrupting the 5V line from USB.

The rear view of the demo in [Figure 3-2](#) shows a [DRV8220EVM](#) is connected to a 227:1 Metal Gearmotor 25Dx56L mm MP 12V that extends the handle via a motor arm. The [DRV8220](#) was selected because it supports phase or enable control and has a relatively small form-factor EVM. A buck converter soldered onto a proto board beside the DRV8220EVM steps the 12V source down to 5V to power the [TI-SCB](#). The TI-SCB then uses an LDO to produce 3.3V. The buck converter allows the demo to operate with only the 12V source, not needing to be plugged into a computer.



Figure 3-2. Rear View of Door Handle Demo

A pair of 3D printed torsion springs help return the handle to the home position after being pressed or pulled, as shown in [Figure 3-3](#). Using springs to pull the handle back instead of the motor helps prevent a pinch hazard.

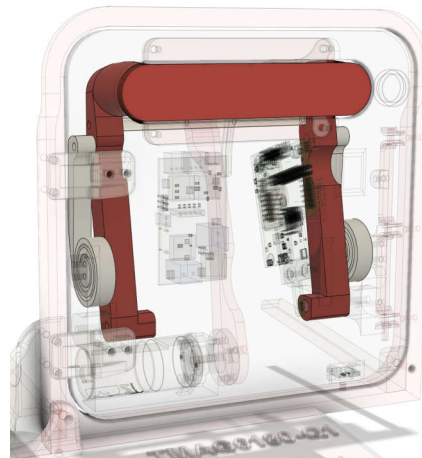


Figure 3-3. Door Handle and 3D Printed Springs

[Figure 3-4](#) shows the [TMAG6180-6181EVM](#) and TI-SCB are mounted on the back-side of the door, and a diametric cylinder magnet is embedded in the handle such that the magnet rotates as the handle rotates.

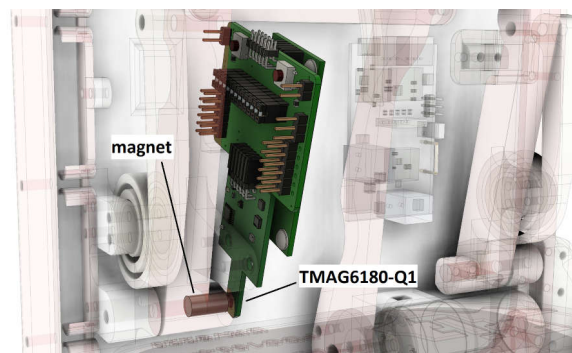


Figure 3-4. TMAG6180-6181EVM, TI-SCB, and Magnet Embedded in Door Handle

The [FDC1004EVM](#) is connected to two capacitive sensors made out of layered copper tape as shown in [Figure 3-5](#).

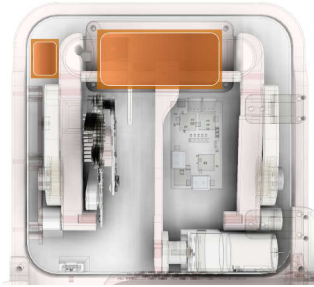


Figure 3-5. FDC1004-Q1 and Capacitive Sensors

[Figure 3-6](#) shows the TMA5131-Q1 mounted on a [HALL-HINGE-EVM](#) board at the bottom of the door, with a small axial cylinder magnet embedded in the door frame.

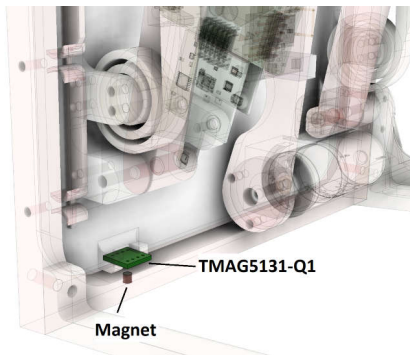


Figure 3-6. TMA5131-Q1 and Magnet Embedded in Door Frame

4 Detailed Design Flow for Door Handle Functions

4.1 Door Open or Closed Detection With Magnetic Sensing

Hall-effect switches are commonly used in transition detection applications, as shown in [Figure 4-1](#). The opening and closing of a car door most resembles the hinge motion, where the magnet swings toward or away from the sensor.

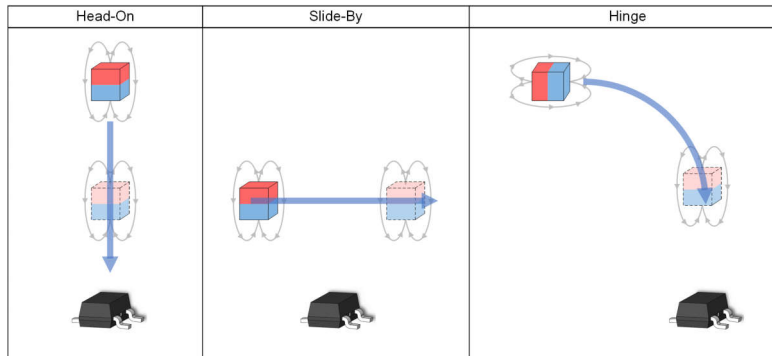


Figure 4-1. Examples of Transition Detection Design Implementations

The magnetic implementation of this function involves embedding the magnet in the door such that the magnet moves in a hinge type motion as the door opens and closes. A Hall-effect switch installed in the door frame opposite the magnet and detects the presence or absence of the magnetic field. Omnipolar switches like the TMAG5131-Q1 can trigger for either North or South magnetic fields as shown in [Figure 4-2](#), whereas unipolar switches can only trigger for one polarity.

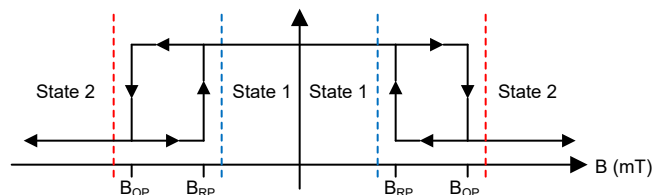


Figure 4-2. Omnipolar Hall-Effect Switch Operation

The main objective is to design the system such that the spatial coordinates of the transition region fall within the spatial coordinates associated with the B_{OP} maximum and B_{RP} minimum specifications.

Important variables to consider when implementing transition detection include magnet size and type, Hall-effect switch selection, and the placement of the magnet and the switch. Magnetic simulation tools like [TI Magnetic Sense Simulator \(TIMSS\)](#) help determine these variables and facilitate rapid design iteration.

4.1.1 Demo Implementation of Open Close Detection Using TMAG5131-Q1

In this demo, a TMAG5131-Q1 automotive Hall-effect switch senses when the door is open or closed. The TMAG5131-Q1 is located on the bottom of the door as shown in [Figure 4-3](#). TMAG5131-Q1 senses the magnetic field from a small magnet embedded in the door frame. The specific device variant is the TMAG5131C1D, which has a sampling frequency of 20Hz, triggers at B_{OP} typical of $\pm 3.0\text{mT}$, releases at B_{RP} typical of $\pm 1.5\text{mT}$, and has 1.5mT hysteresis. The digital output from this device goes to an input pin on the TI-SCB.

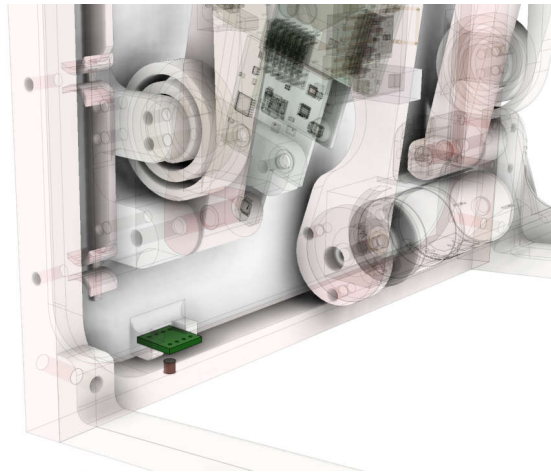


Figure 4-3. TMAG5131-Q1 Placement and Magnet Embedded in Door Frame

The TMAG5131-Q1 is centered above the magnet, with a 4.08mm airgap between the top of the sensor package and the surface of the magnet. The magnet and sensor are each around 140mm away from the hinge origin. The magnet has a height of 3.08mm and radius of 1.59mm.

Figure 4-4 shows the simulation result from TI Magnetic Sense Simulator (TIMSS) for these magnet and sensor locations over a 90 degree rotation from closed to open. The simulation is configured to consider the TMAG5131-Q1 B_{OP} max and B_{RP} min, which helps to identify the worst case for when the device can change states. The results show that the TMAG5131-Q1 output releases after 3 degrees of rotation as the door is opened. As the door is closed, the TMAG5131-Q1 output activates at 2 degrees. These magnetic transitions are within the spatial bounds of the door in the closed position and open position, which is considered to be 90 degrees in this case. A transition region between 2 to 3 degrees helps ensure the TMAG5131-Q1 releases even if the door is only opened slightly, and that the TMAG5131-Q1 only activates again when returned to the closed position.

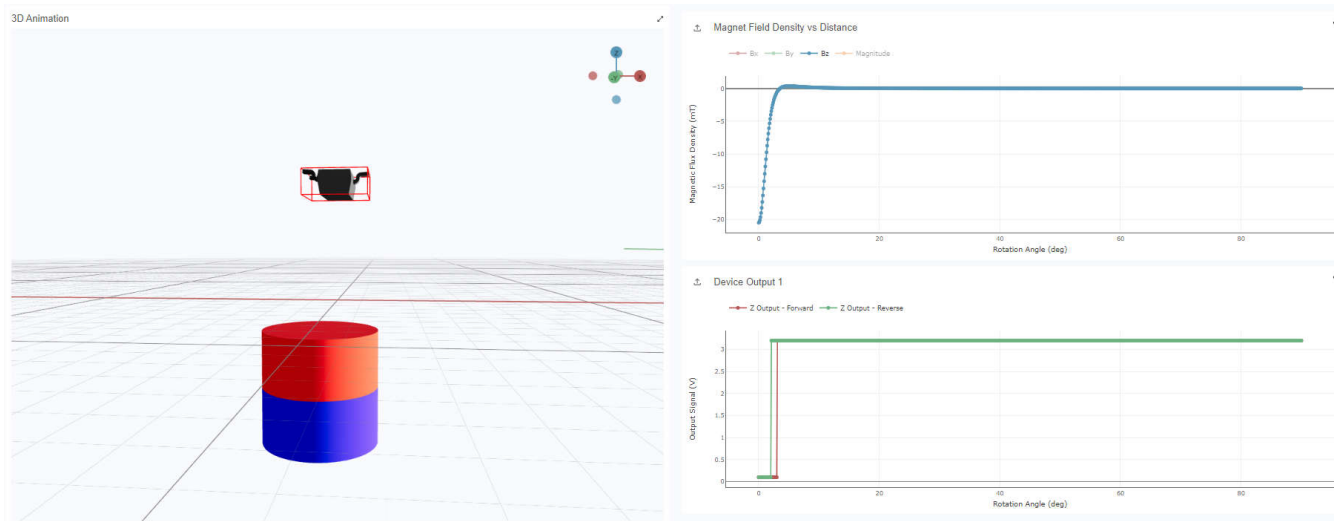


Figure 4-4. TMAG5131-Q1 Door Open or Closed TIMSS Simulation Results

In the GUI for this demo, a GPIO on the TI-SCB monitors the output of the TMAG5131-Q1 to determine whether the door is open or closed and displays the current state using the door indicator. In Figure 4-5 and Figure 4-6, you can see the door indicator is closed when the door is closed, and illuminates when the door is opened. The full operation of the door open or closed detection in the demo is shown in this [video](#).



Figure 4-5. Door Closed Indicator

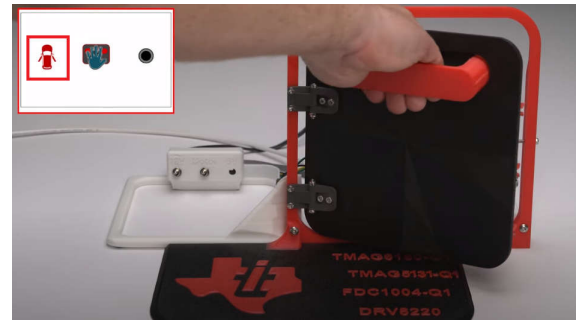


Figure 4-6. Door Open Indicator

4.2 Deployable Door Handle Position Detection With Magnetic Sensing

Tracking the position of a deployable door handle as the door handle is extended and retracted can be achieved in several different ways using magnetic sensing. The movement of the handle can be tracked as either linear motion or a rotation motion. For the purposes of this application note, we consider the rotation of the handle on the axis as the handle is extended and retracted, as shown in Figure 4-7.

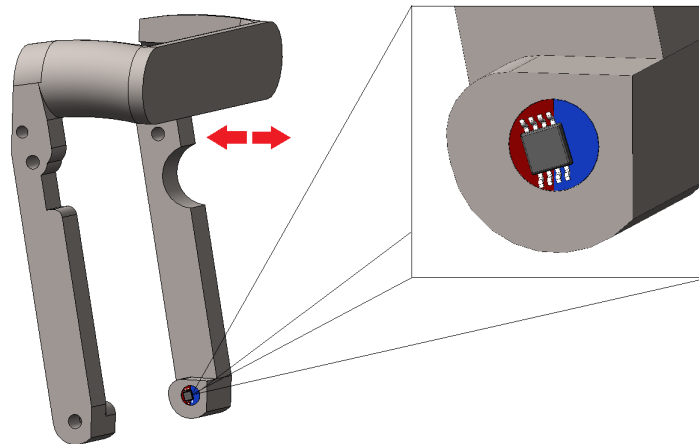


Figure 4-7. Door Handle Rotation Motion

A diametric cylinder magnet can be embedded in the deployable door handle such that the magnet is centered and rotates on the same axis as the handle itself. Thus, the angle of the magnet changes as the door handle extends and retracts. An AMR angle sensor or 3D-linear Hall-effect sensor can be placed on-axis with the magnet or off to the side in an off-axis position, as shown in Figure 4-8.



Figure 4-8. On-Axis vs. Off-Axis Sensor Alignment

The sensor detects the angle of the magnetic field as the magnet rotates. For an accurate angle measurement, the two axes' amplitudes must be normalized. For an on-axis alignment, typically the amplitudes are well-matched, as shown in Figure 4-9. Off-axis topologies often result in an amplitude mismatch between the two

axes, as shown in Figure 4-10. Devices like the TMAG5170-Q1 and TMAG5173-Q1 offer an on-chip gain adjustment option to account for amplitude mismatch and mechanical position misalignments.

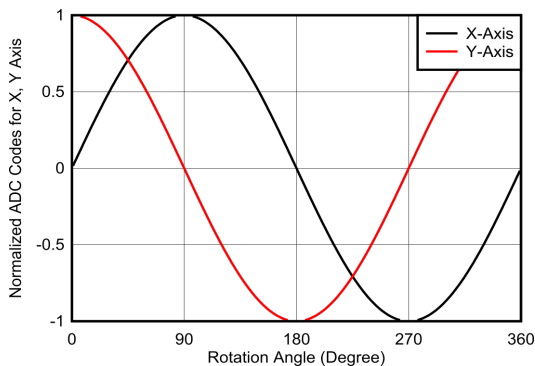


Figure 4-9. Sensor Data for 360° Rotation With On-Axis Alignment

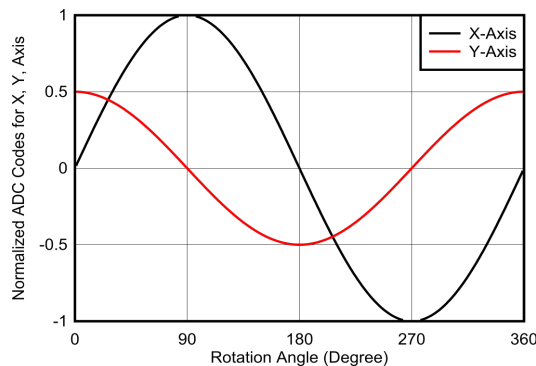


Figure 4-10. Sensor Data for 360° Rotation With Off-Axis Alignment

Depending on what kind of sensor is chosen, the magnetic output signals can be analog or digital signals. With two signals that have well-matched amplitude and are 90° out of phase, the angle can be calculated using the arctangent function shown in Equation 1.

$$\theta = \text{atan2}\left(\frac{B_X}{B_Y}\right) \tag{1}$$

Where:

- θ represents the angle of the magnetic field
- B_X represents the magnitude of the X component of the magnetic field vector
- B_Y represents the magnitude of the Y component of the magnetic field vector

In this example, the X and Y components of the magnetic field vector are used. Depending on sensor placement, it can be appropriate to use the X and Z or Y and Z field components for the angle calculation instead.

Some devices, such as the TMAG5170-Q1 and TMAG5173-Q1, offer an integrated CORDIC that provides full 360° angle position information for both on-axis and off-axis angle measurement topologies. With a reliable and accurate angle measurement from the magnet, changes in the angle are then correlated to the handle position as it deploys, retracts, is pulled or is pushed for proper state detection.

4.2.1 Demo Implementation of Deployable Door Handle Position Sensing Using TMAG6180-Q1

In this demo, a TMAG6180-Q1 automotive high-precision analog AMR angle sensor with 360 degree angle range is used to monitor handle position. A diametric magnet is embedded in the handle assembly and centered on the handle's axis of rotation, as shown in Figure 4-11. The TMAG6180-Q1 is mounted so that the AMR sensing element is centered in an on-axis alignment, with the top of the TMAG6180-Q1 about 1.5mm away from the surface of the magnet. The magnet has a height of 12mm and a radius of 3.18mm. The handle is roughly 98.52mm away from the axis of rotation, meaning that for each degree of rotation, the handle moves about 1.72mm.

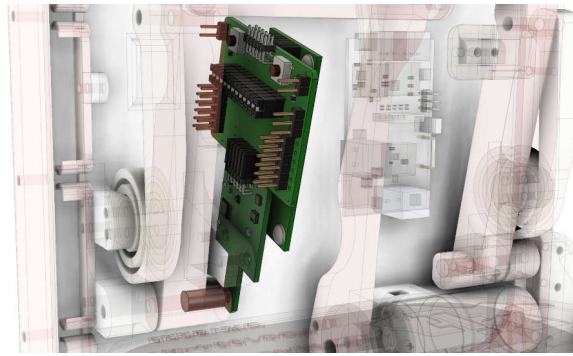


Figure 4-11. TMAP6180-Q1 Placement and Magnet Embedded in Handle

Figure 4-12 shows the simulation results from TI Magnetic Sense Simulator (TIMSS) for these magnet and sensor locations over a 360 degree rotation. The first plot shows the changing X and Y vectors of the magnetic field as the magnet rotates. With the amplitudes well-matched due to the on-axis alignment. The second plot shows the changing differential sine and cosine analog outputs from the TMAP6180-Q1. Notice that for every 360 degree rotation of the external magnetic field, the AMR outputs provide two periods. This is because the outputs have an electrical range of 180. If the mechanical angle between the sensor reference and the direction of the magnetic field is θ , then the AMR outputs correspond to $\cos(2\theta)$ and $\sin(2\theta)$ respectively. By utilizing the digital outputs of the Hall sensors shown in the third plot, the angle range of the AMR sensor can be extended to 360 degrees. Mechanical tolerances can also be simulated in TIMSS using the parametric sweep feature to see the potential impact on angle measurements.

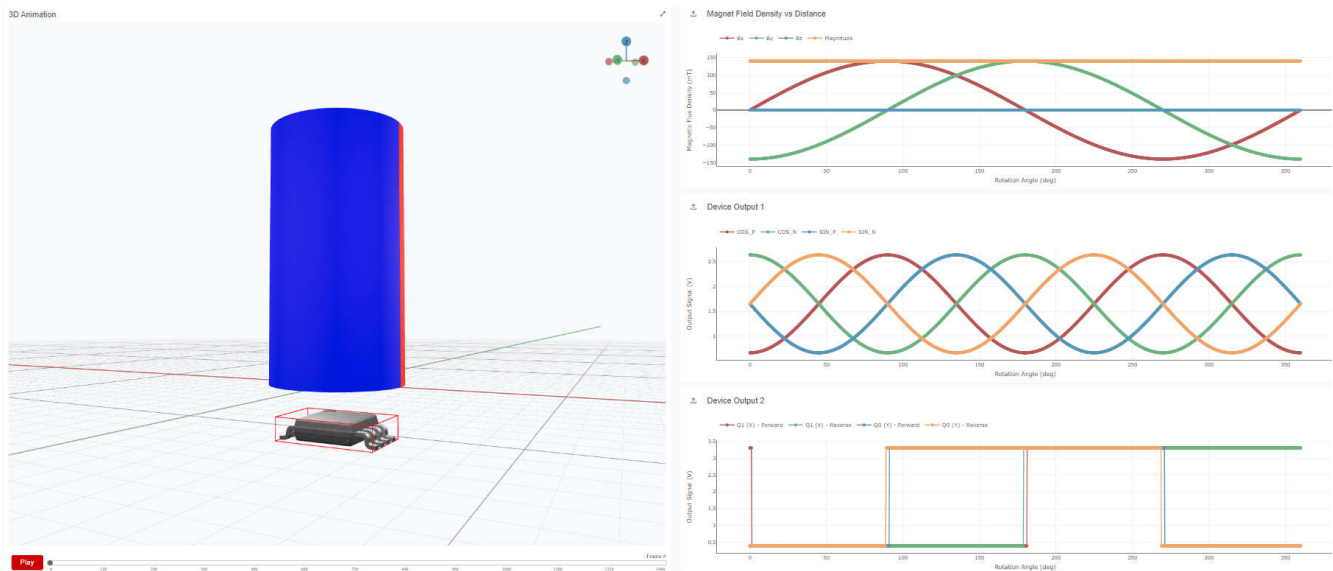


Figure 4-12. TMAP6180-Q1 TIMSS Simulation Results

In the GUI for this demo, the sine and cosine outputs of the TMAP6180-Q1 and the Q0 and Q1 outputs are used in an arctan2 calculation to determine the handle's angle of rotation.

The angle plot in Figure 4-13 shows the handle angle measured by the TMAP6180-Q1 over time. In the demo, the handle angle measures approximately 56° when the handle is resting in the door, and approximately 46° when fully driven out by the DRV8220. The handle is driven out 17.4mm away from the door, which supports the previous calculation that the handle is extended roughly 1.72mm for each degree of rotation.

These angle limits can be adjusted if the user desires the handle to be deployed more or less. Additionally, the handle measures approximately 59° when pressed in by the user and approximately 45° or less then pulled by the user. These angle measurements make it easy to implement other functions that are initiated when the handle is pressed, or to ensure the handle does not retract while a user is pulling on the handle. The full operation of deployable door handle position detection in the demo is shown in this [video](#).

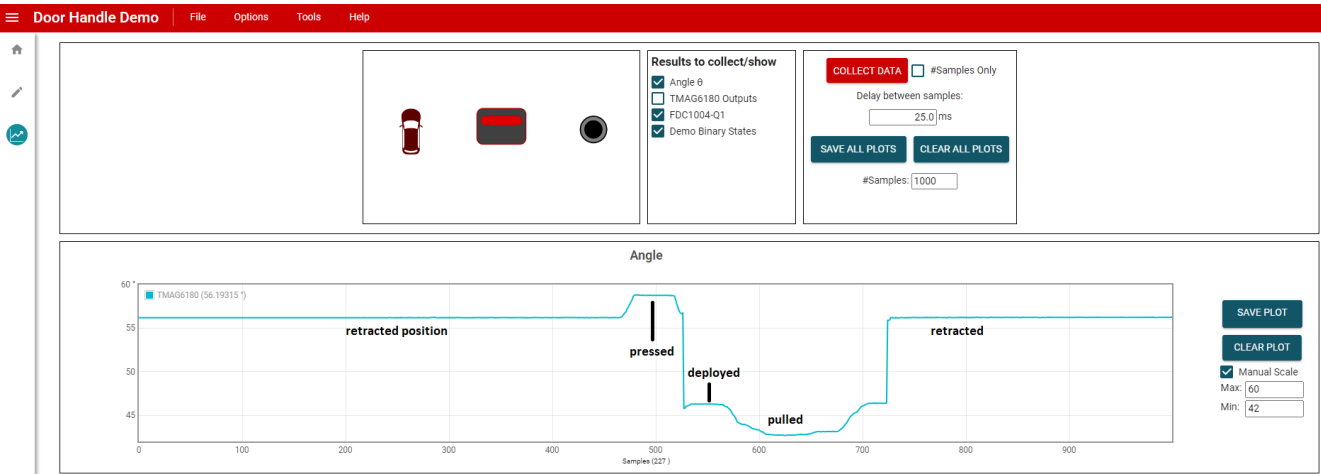


Figure 4-13. Door Handle Angle of Rotation Plot

4.3 Hand Proximity Detection With Capacitive Sensing

4.3.1 Overview of Capacitive Sensing Applications

Capacitive sensing is a technology that senses the distortion of a sensor electrode's electric field by an external target (object to be measured). The sensor electrode is frequently a conductive structure (like a copper plate) that radiates an electric field onto the target, forming a mutual capacitance between the sensor electrode and the target. The capacitive sensor device (in this case the FDC1004) detects the capacitance change, and provides output data that reflects the new capacitance value.

Figure 4-14 illustrates how capacitive sensing can be used in proximity detection, liquid level sensing, and material detection. In proximity detection - emphasized in this application note - a grounded, conductive object, like the finger shown in the left diagram, is effectively a ground plane and forms a mutual capacitance with the sensor. As the finger moves toward or away from the sensor, the capacitance changes, which is then detected by the capacitive sensing device. In liquid-level sensing, the positions of the sensor and target (the liquid) are fixed, and the changes in liquid level cause the sensor or liquid capacitance to change, which is detected by the device. In material detection, the sensor and target can have fixed size and positions, and the sensor or target capacitance can help distinguish different materials through the target materials' permittivity ($\epsilon_t = \epsilon_r \epsilon_0$) and the impact on capacitance. For more detailed information, please see [FDC1004: Basics of Capacitive Sensing and Applications](#).

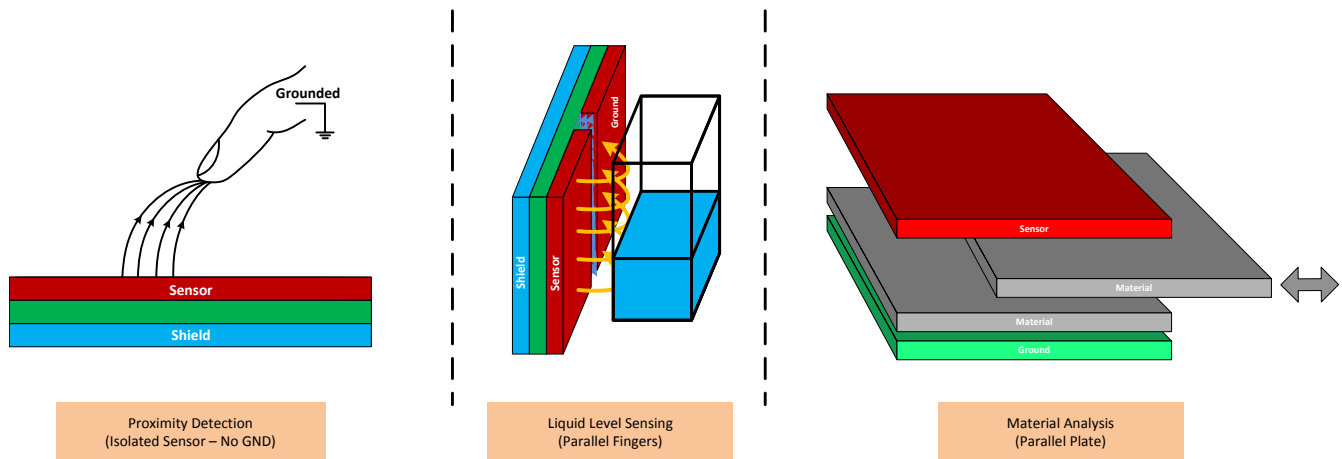


Figure 4-14. Capacitive Sensing Applications

Two challenges with capacitive sensing are interference from nearby objects and electromagnetic (EM) energy in the surrounding environment. Both can frequently be managed by sound mechanical design and the use of *active shields*. Active shields offer an advantage over grounded shields in that they can be positioned close to

the sensor for maximum protection without adversely loading the sensor and overwhelming the measurement of the target's capacitance. Unlike grounded shields, which are by definition held at zero voltage, active shields are driven with the same waveform as the sensor, so there is no voltage difference between the sensor electrode and the active shield. The zero voltage difference between the sensor and shield waveforms will avoid loading of the sensor by the nearby shield. The low output impedance of the shield driver will attenuate external EM fields incident on the shield, and isolate the sensor from nearby objects. The active shield will help focus the region of detection to the unshielded side of the sensor.

A shield electrode can be paired with the sensor electrode in several ways, as shown in [Figure 4-15](#).

- A shield the *same size* as the sensor electrode placed directly underneath the sensor.

This configuration represents the minimum shield size that needs to be used.

- A shield *larger than the sensor* electrode placed directly underneath the sensor. Compared to *same-size* sensors, this provides better attenuation of interference from sides below the sensor
- A *shield ring* wrapped around the top side adjacent to the sensor with a shield underneath the sensor. This provides the best attenuation of interference originating from below and to the sides of the sensor.

The distance between the sensor and shield electrode needs to be minimized to make sure the best attenuation of interference with respect to the sensor electrode.

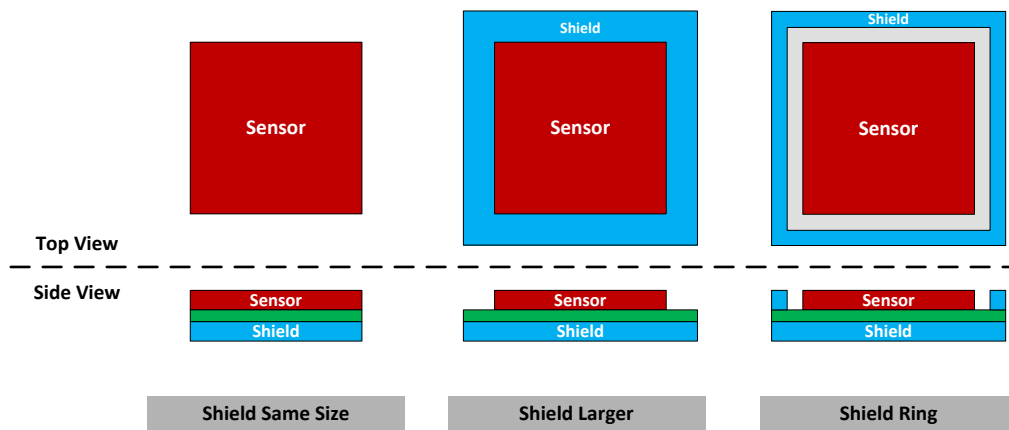


Figure 4-15. Active Shield Configurations

Note that PCB traces connected to the sensor electrode can also be sensitive to interference. Depending on the design and PCB layout, it may be possible to shield the PCB traces that connect to the sensor, thereby attenuating interference on the traces. For more detailed information, please see [Capacitive Sensing: Ins and Outs of Active Shielding](#).

The designs of the sensor electrode can vary widely, and are often dependent on the mechanical constraints of the system. General guidelines are difficult to provide, and a final sensor design can frequently come down to trial-and-error and perhaps (but not always) EM simulations. A good starting point for a touch detection application is to consider the well-known equation for a designed for parallel-plate capacitor:

$$C = \frac{\epsilon_r \times \epsilon_0 \times A}{d} \quad (2)$$

Where:

- A = area of the two plates (meters²)
- ϵ_r = relative permittivity of the material between the two plates
- ϵ_0 = permittivity of free space, 8.85×10^{-12} F/m
- d = separation distance between the plates (meters)

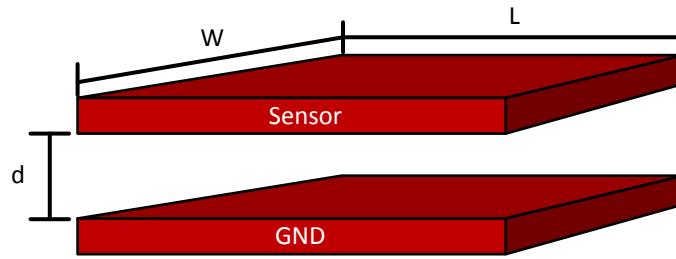


Figure 4-16. Parallel Plate Capacitor

A good starting point is to consider the available sensor area due to mechanical requirements, and use [Equation 2](#) to approximate the resulting capacitance. For a car door handle in resting position (for example, with no nearby hand), the sensor electrode could have curvature or contours, and the effective ground plane could be a combination of surfaces with different distances, making straightforward calculations difficult. Add to this the fact that other materials - with permittivity ($\epsilon_T = \epsilon_r \epsilon_0$) - can be positioned between the sensor and ground electrodes, as could moisture and other contaminants, and all of these can affect the capacitance. This inactive state can be important because it establishes the nominal, *resting* capacitance of the sensor.

If the car door handle is being activated, the nearby hand needs to be the dominant ground surface, and can have more or less area than the sensor. If the area of the hand or fingers is larger than the sensor, then [Equation 2](#) offers a sound approximation. If the hand or finger area is less than the sensor, then the actual sensor capacitance can likely be less than predicted by the equation.

More detailed information is available in the [Capacitive Proximity Sensing Using the FDC1004](#), application note.

4.3.2 Examples of Soft-Touch Detection Based on Capacitive Sensing in a Door Handle Demo

While the last section gave an overview of capacitive sensing, this section can provide an example of capacitive sensor design used in a [Figure 4-17](#), and in the associated [Position Sensing in Automotive Door Handle Systems](#), application brief. [Figure 4-17](#) shows a photo of the door handle demo, which uses capacitive touch detection for two functions. One function is a soft touch *button* that allows the user to lightly touch a designated surface on a car door, which in turn unlocks and or opens the door. In the door handle demo, this touch surface is located just to the right of the pop-out door handle. This *touch* function is in contrast to the more familiar *push-button* that requires some small force of actuate the button function (covered in a subsequent section of this application note). The second use of capacitive sensing in the demo is to detect the presence of a hand inside the pop-out door handle which can then allow the door to open and also keep the door handle from retracting back into the door surface.

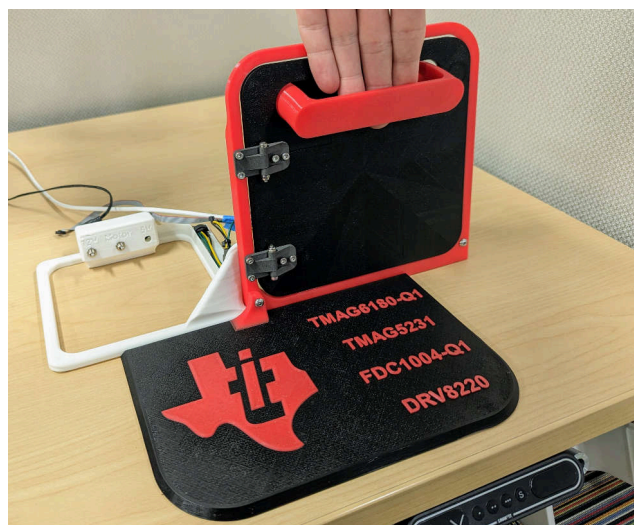


Figure 4-17. Car Door Handle Demo

How are the capacitive sensors implemented in our door handle demo? Figure 4-18 shows a virtual rendering of the back side of the demo, with the capacitive sensors displayed as copper-colored rectangles in the upper fourth of the image. The small rectangular sensor on the left is used to detect the increased capacitance due to a user's finger touching the designated touch-button surface to the right of the door handle on the outside surface. The larger rectangle is positioned on the inside surface of the cavity used to accommodate the retracted door handle. The large rectangular sensor is used to detect the increased capacitance due to the presence of a user's fingers on the inside surface of the popped-out handle. The demo housing is a polycarbonate resin with a relative permittivity of five ($\epsilon_r = 5$) with respect to free space.

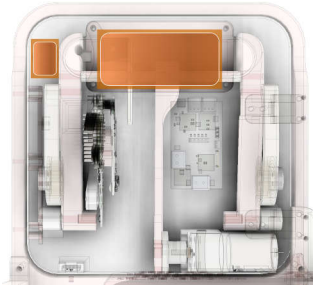


Figure 4-18. Back Side of Car Door Handle Demo with Copper Capacitive Sensors Highlighted

The capacitive sensors were developed with a little-trial-and-error, but it is possible to get close on a first try using the parallel plate equation given in Equation 2.

In the following analysis for the touch button and the door handle, we assume the user's fingers or hand act as a ground plane with respect to the sensors located on the inside surface of the door. The fingers or hand serve as the secondary *plate* in capacitor equation shown in Equation 2. We make the additional simplifying assumption the finger or hand present an area identical to the sensor on the inside surface of the door.

4.3.2.1 Touch Button

Consider the touch button located to the (outside) right of the pull handle (to the left on the inside). The 1.4cm x 2.1cm rectangular sensor is positioned on the inside surface of the 5mm-thick polycarbonate plastic. If we assume this condition can be approximated by an idealized parallel-plate capacitor, we can expect the capacitance to be about $C \approx \epsilon_0 \epsilon_r A/d = 8.85 \cdot 10^{-12} \cdot 5 \cdot (0.014) \cdot (0.021)/0.005 = 2.17\text{pF}$ when a finger is pressing against the outer surface. This assumes the area of the finger pressing the outer surface is at least as large as the sensor on the inside surface of the polycarbonate.

We also might approximate the absence of any finger on the touch button as a parallel-plate capacitor with a separation distance much larger than the sensor dimensions. Following this assumption, suppose the distance d is 30mm. This can result in a capacitance of $C \approx \epsilon_0 \epsilon_r A/d = 8.85 \cdot 10^{-12} \cdot 5 \cdot (0.014) \cdot (0.021)/0.030 = 0.43\text{pF}$.

How do these two approximate calculations compare to the demo? The plot in Figure 4-19 shows a plot of the demo's FDC1004 output versus time samples with a finger placed over the touch button between the 400th and 500th sample. Before the finger is applied, the FDC1004 reports the sensor capacitance is about 0.5pF to 0.6pF, which somewhat in agrees with our rough calculations. After the finger is placed over the button, the reported capacitance settles out to 2pF to 2.1pF, which is close to values from our approximate calculations above.

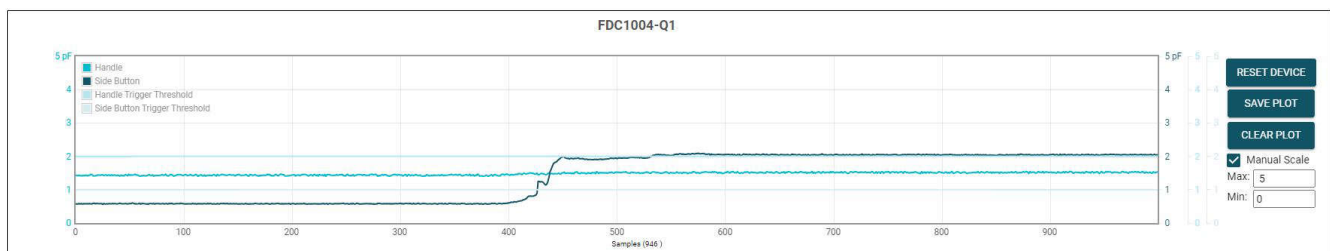


Figure 4-19. Demo Touch Button: FDC1004 Reported Capacitance Before and After Finger is Applied

4.3.2.2 Door Handle

Even an approximate analysis for the door handle in the retracted and extended positions is a little more complicated because of air gaps and plastic between the sensor, the outer surface and the user's hand. Some simple calculations - similar to the touch button - but considering the permittivity effects of plastic and air gaps, combined with the parallel plate capacitor equation in Equation 2, can arrive at results that are very close to our experimental results using the demo. To that end, we can specify the thicknesses of the plastic and air gaps for the case of a hand on an extended handle.

The mechanical stack-up (showing widths of air gaps and thicknesses of plastic) is shown in Table 4-1 and Figure 4-20.

Table 4-1. Mechanical Stackup Between Door Handle and Capacitive Sensor

Handle Sensor Dimensions	Width = 8cm, Height = 5cm
1. Plastic thickness between door handle sensor and chamber that houses retracted handle	2mm
2. Distance between chamber outer surface and door handle outer surface (air gap)	10mm

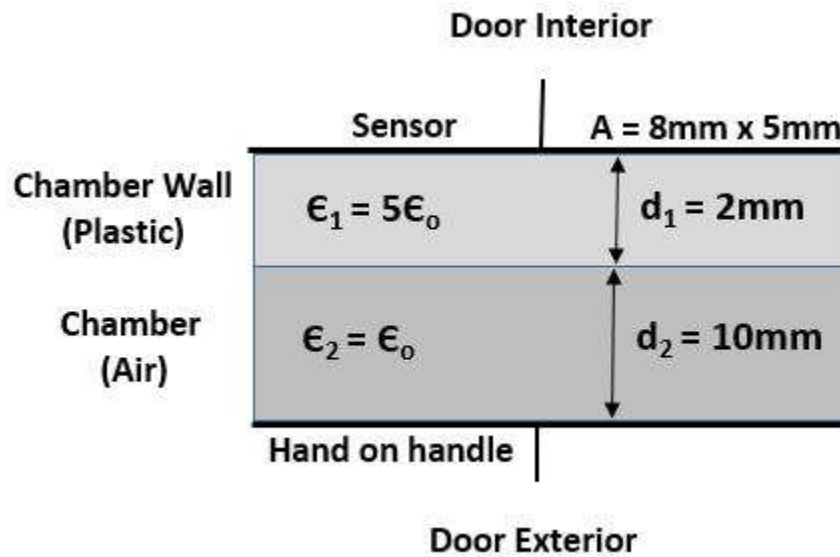


Figure 4-20. Door Handle Mechanical Stack-up For Calculating Capacitance

What are the approximate capacitance can we expect with the previous stack-up using the parallel capacitor equation given earlier? Consider a hand gripping the extended handle as shown in Figure 4-21.

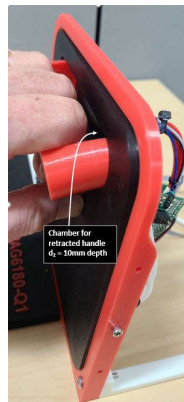


Figure 4-21. Hand Gripping Extended Handle

Consider that items (1) and (2) in [Table 4-1](#) are really the only distances we need to consider for our capacitor equation. First, item (1) is the 2mm-thick plastic ($\epsilon_r = 5$) between the door 8cm by 5cm door handle sensor and the chamber that houses the retracted door handle. The second, item (2) is the 1cm air gap ($\epsilon_r = 1$) between the outer surface of the 2mm-thick plastic and the outer surface of the door. When a hand grips the extended handle, the user's fingers can form a ground plane that can be about 1cm from the chamber's outer surface (per item 2 above).

So for our capacitor, one parallel plate can be the sensor, and the other can be the ground plane formed by the user's fingers gripping the door handle. If we make the simplifying assumption the surfaces of the two planes are equal, and our total capacitance can be approximated by a region with two different permittivity, as shown in [Figure 4-20](#).

The total capacitance between the sensor and the users fingers can be approximated as two capacitors in series that have the same *plate* areas, but different gap lengths and permittivity. The quantities based on our stack-up are based on the plastic [$d_1 = 2\text{mm}$, $\epsilon_{r1} = 5$] and the air gap [$d_2 = 1\text{cm}$, $\epsilon_{r2} = 1$] between the chamber's surface and the user's fingers are summarized in the following equation.

$$\frac{1}{C_T} = \frac{1}{C_1} + \frac{1}{C_2} = \frac{d_1}{\epsilon_1 A} + \frac{d_2}{\epsilon_2 A} \quad (3)$$

$$C_T = \frac{\epsilon_1 \epsilon_2 A}{\epsilon_2 d_1 + \epsilon_1 d_2} = \frac{\epsilon_{r1} \epsilon_{r2} \epsilon_o^2 A}{\epsilon_{r2} \epsilon_o d_1 + \epsilon_{r1} \epsilon_o d_2}$$

$$C_T = \frac{\epsilon_o \epsilon_{r1} A}{\epsilon_o d_1 + \epsilon_{r1} d_2} = \frac{5 \epsilon_o (0.08 \times 0.05)}{(0.002) + 5(0.01)}$$

$$C_T = 3.4\text{pF}$$

How does this simple calculation compare with results from the demo? [Figure 4-22](#) shows a plot of the demo's FDC1004 output versus time samples with a hand gripping the deployed handle between the 400th and 500th time samples. Before the hand grips the handle, the FDC1004 reports the sensor capacitance is about 1.5pF, which somewhat in agrees with our rough calculations of 1pF. After a hand grips the handle, the reported capacitance settles out to about 2.9pF. While this is not the calculated value, it does reflect the fact the surface of the hand closest to the sensor is around 12mm to 13mm, not the 10mm used in our calculations.

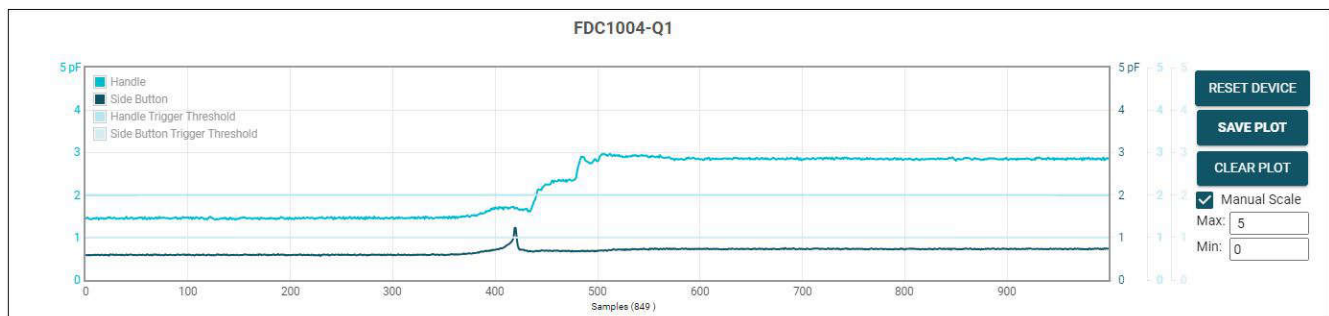


Figure 4-22. Demo Door Handle: FDC1004 Reported Capacitance Before and After Gripping the Handle

4.4 Push Button With Inductive Sensing

4.4.1 Inductive Push Buttons

Inductive sensors operate on the principle of resonance between a variable inductor in the form of a sense coil, and a fixed, lumped-element (PCB) capacitor as illustrated in the following. The fixed capacitor and inductive coil form the external LC tank circuit required for LDC operation. The tank circuit resonates at a frequency dependent on the sense coil inductance and the fixed capacitance:

$$f_{res} = \frac{1}{2\pi\sqrt{LC}} \quad (4)$$

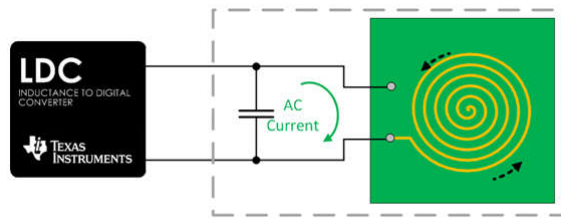


Figure 4-23. Inductive Sensor Theory of Operation

The inductance of the sense coil varies in response to a nearby conductive object, which causes a shift in the LC tank resonant frequency, which the inductive sensing device (LDC) subsequently detects. For more information on inductive sensors, please see the [Inductive Sensing Overview](#) video, or the [Common Inductive and Capacitive Sensing Applications](#), application note.

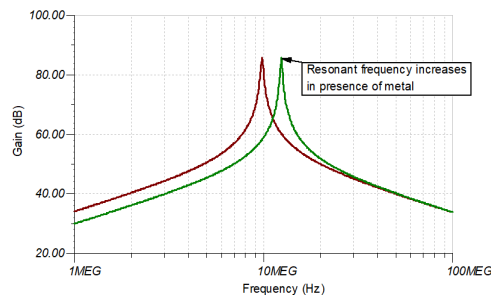


Figure 4-24. Inductive Sensor Shift in Resonant Frequency in Response to Target Movement

Push-button applications have long been implemented with mechanical switches that force electrical contacts together and (hopefully) make a low resistance connection. Even with their long history, mechanical switches can be prone to environmentally-induced failures, as well as wear-and-tear. Harsh environments can lead to intrusion and contamination (via dirt, oil, water, and so on) and can require special housings, gaskets, and other fittings to avoid premature failure. Robust, sealed mechanical switches that are resistant to contaminants are achievable, albeit at increased cost.

Push-button switches based on inductive sensing (LDCs) show very few of these shortcomings. The switches are robust and not subject to the inevitable failures associated with moving parts and worn contacts due to wear-and-tear from repetitive movement. The switches can be easily made immune to contaminants, and maintain reliability even in wet environments. The switches can accommodate spacious form-factors (to support users with gloves) or small form factors for limited space.

Some devices and designs can also support multilevel push buttons, and some have internal algorithms to manage multiple button-presses as well as mechanical distortions, freeing the microcontroller from managing those functions.

Inductive touch-buttons can be easily implemented with three main components: an inductive sensor, a target surface, and an inductance-to-digital converter (LDC). The sensor can frequently be implemented by a PCB-based or flex-circuit based coil. The target can be a flexible, conductive material, like thin metal with enough thickness to support skin-effect eddy currents.

As shown in [Figure 4-25](#), a force applied on the target surface causes the material to deflect slightly, reducing the distance (D_{TARGET}) between the inductive sensor and the target surface. The deflected conductor reduces the sensor inductance, which in turn causes the sensor resonant frequency to increase which is detected by the LDC. As a target deflection example, with an applied force of 1 Newton, a button with a 20-mm diameter can deflect about 0.1 μ m if the target material is 430 stainless, 1-mm thick. When the force is removed, the button surface returns to the original shape.

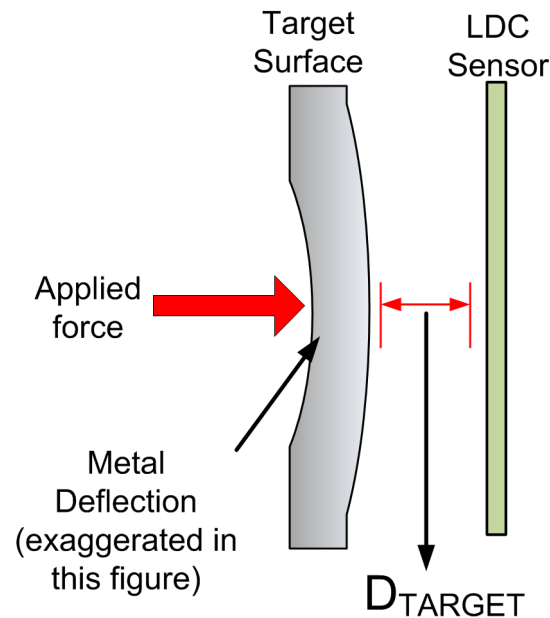


Figure 4-25. Inductive Touch Button Components

4.4.2 Inductive Push Button Sensitivity

The primary factors that contribute to the sensitivity of an inductive touch button are the [target material and thickness](#), the [target distance](#) (D_{TARGET} in [Figure 4-25](#)), and the [LDC sensor size](#). Button sensitivity is defined in terms of force that needs to be applied on the target conductive surface to trigger the desired LDC response.

4.4.3 Target Material

A material with higher electrical conductivity (σ) - such as copper, aluminum or silver - is a better target for inductive sensing technologies because the amount of eddy currents generated on the target are directly related to conductivity (σ) of the target material. A thin layer of conductive material can be added on to non-conductive materials like plastic to make effective targets for push-button applications. [Figure 4-26](#) illustrates the sensitivity of the LDC to the conductivity of the material through the dependence of the sensor frequency shift (which the LDC detects) on the target material and the sensor frequency (which impacts the skin effect). Note the two best conductors - copper and aluminum - give the greatest frequency shift over all sensor frequencies. The [LDC Target Design](#) application note provides additional details, and the spreadsheet-based [LDC Sensing Design Calculator Tool](#) lets you calculate and model the effects of target conductivity and thickness.

A thinner or less rigid target material requires less force than a thicker or more rigid one. The [spreadsheet tool](#) also allows you to model the deflection produced in the target surface with a given amount of force that is inversely proportional to the tensile strength and thickness of the material. If we modify our previous example (target: 20mm diameter, 1mm thick) to a thickness of 0.5mm, the target deflection under 1 Newton of applied force increases from 0.1um to 0.880um. Please be sure to check the desired target thickness against the eddy current depth through the tool's *SkinDepth* tab. If a target is too thin to support approximately 3 skin depths, it can degrade the button sensitivity.

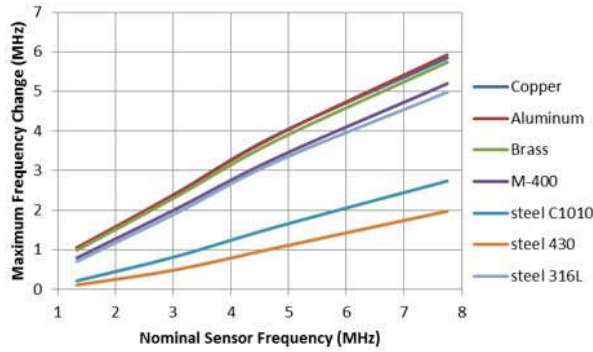


Figure 4-26. Target-Induced Frequency Shift vs Nominal Sensor Frequency with Target Material as a Parameter

4.4.4 Target Distance and Sensor Size

Inductive sensing relies on the interaction of EM fields generated by the inductive sensor and the eddy currents being induced on the conductive surface. The amount of eddy currents induced on the target surface decrease with an increase in D_{TARGET} as the target conductive surface now captures a smaller portion of the electromagnetic field being generated by the inductive sensor. In turn, the size of electromagnetic field lines generated by an inductive sensing coil is directly proportional to the diameter of the sensor. Figure 4-27 shows how to set D_{TARGET} as a percentage of the coil diameter for inductive touch. As Figure 4-27 shows, the best switch sensitivity happens when the D_{TARGET} is within 20% of the diameter of the sensor coil. This can support push buttons with > 1um of target deflection.

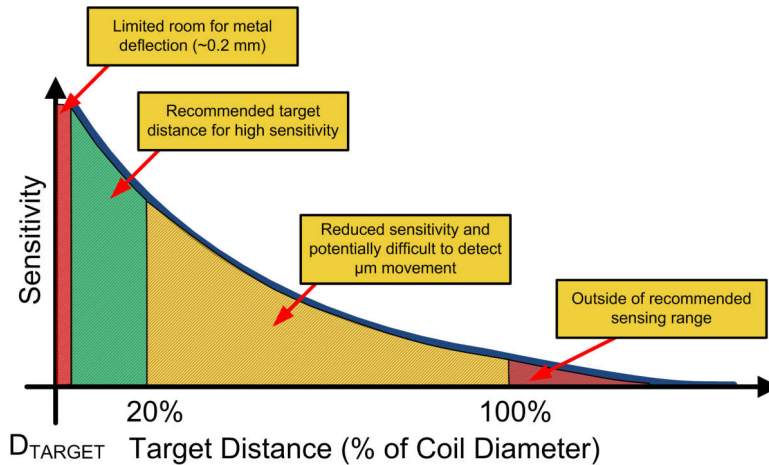


Figure 4-27. Button Sensitivity as a Function of Target to Sensor Distance (D_{TARGET}) as a Percentage of the Sensor Coil Diameter

4.4.5 Design Example

For this design example, we can assume the button is contained within a dedicated plastic housing, with a PCB and metal tape to provide a target surface. The [Inductive Sensing Calculator Tool](#) was used to help determine the coil parameters for this example. [Figure 4-28](#) shows an image of the *Spiral_Inductor_Designer* tab used for the entries that follow. The numbers ((#)) track the steps and correspond to the numbers in blue font (#) on the left side of [Figure 4-28](#).

- The number of coil PCB layers was assumed to be two, so the tool's *Layers* field (1) in [Figure 4-28](#) was set to two.
- The *Sensor Shape* (2) was chosen to *Circular*
- The *Outer diameter of the inductor* (3) was set equal to 8mm.
- *Spacing between traces*(4) and
- *Width of trace* (5) was set to 5mils
- *Turns per layer* (6) was set equal to eight.
- These settings result in an *Inductor inner diameter* (7) slightly less than 4mm with a resulting *Coil Fill Ratio* (8) (inner diameter divided by outer diameter) of roughly 50%. For most button designs, minimizing the coil fill ratio can provide additional sensitivity but requires the target surface to be very close to the coil for it to be beneficial. Otherwise, it is best to keep the coil fill ratio between 20% and 80% to maximize the Q factor of the design.
- For this design the resulting *Q factor* (9) is equal to 37 with no target (for example, button surface not present).
- The *Sensor capacitance* (10) for this sensor design was selected to be 220pF which put the *Sensor Operating Frequency no target* (11) interaction at 8.396MHz.
- Based on the coil diameter, a (button pressed) *Target Distance* (12) of 0.8mm away from the coil was selected. This puts the target well within the recommended 3%-20% range of the coil diameter which can give a high sensitivity in response to a force on the button surface.
- As the spreadsheet shows, a *Target Distance* of 0.8mm results in a *Sensor Frequency with Target Interaction* (13) of 11.081MHz with a *Q factor* (14) of 26

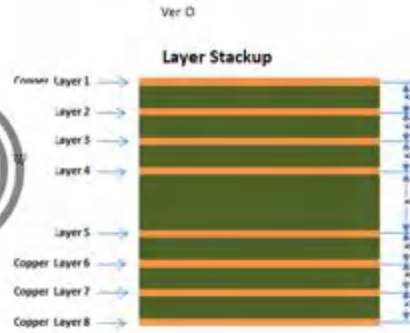
The spreadsheet can give a warning if any of the final parameters are out of range for the device, but in this case, no warnings appear.

Note the tool supports many inductive sensors, and the sensors can be selected by the pull-down menu in the *LDC Device* field. The tool tailors the notifications and warnings to each device's parameters and specs and features.

TI LDC Inductance Calculator

Estimator tool for racetrack spiral coils. This tool is provided without warranty or support. User assumes all liability.
[Take a look at this blog post for additional information](#)

[Return to Main page](#)



Enter only in Yellow Fields (pull-down for mm or mil)
Results in Orange Fields



←Double-Click For Instructions

LC Sensor calculations				
LDC Device		LDC3114		
Operating temperature	T	25 °C		Enter operating temperature
(10) Sensor capacitance	C	220.0 pF		Select LC tank capacitance
(1) Layers	M	2 Layers		Number of layers on PCB board (1≤M≤8)
(6) Turns (per layer)	N	8 Turns		Number of turns per layer
(3) Outer diameter of the inductor	d _{OUT}	8.00 mm		Outer Diameter of the spiral inductor
(2) Sensor Shape		Circular		
Long side of inductor	d _l	20.00 mm		
(4) spacing between traces	S	5.000 mil		Space between traces (mm or mil)
(5) width of trace	w	5.000 mil		Width of the trace (mm or mil)
PCB thickness between 1st layer and 2nd layer	h12	8.000 mil		Space between layer 1 and 2 (mm or mil)
PCB thickness between 2nd layer and 3rd layer	h23	30.000 mil		Space between layer 2 and 3 (mm or mil)
PCB thickness between 3rd layer and 4th layer	h34	8.000 mil		Space between layer 3 and 4 (mm or mil)
PCB thickness between 4th layer and 5th layer	h45	8.000 mil		Space between layer 4 and 5 (mm or mil)
PCB thickness between 5th layer and 6th layer	h56	8.000 mil		Space between layer 5 and 6 (mm or mil)
PCB thickness between 6th layer and 7th layer	h67	1.575 mil		Space between layer 6 and 7 (mm or mil)
PCB thickness between 7th layer and 8th layer	h78	1.575 mil		Space between layer 7 and 8 (mm or mil)
Copper thickness	t	1.000 oz-Cu		Copper layer thickness (mm,oz-Cu, or mil)
Conductor Resistivity (at 20°C)	pr	1.68E-08 Ωm		Use 1.68E-08 for Copper
Conductor Resistivity temperature coef	pr_tc	0.393 %/°C		Use 0.393 for Copper
Conductor relative permeability	μ	1.00		Use 1.0 for Copper
Parasitic capacitance	C _{par}	4.0 pF		Estimate - generally in the rage of 1 to 5 pf
Copper resistivity at operating temperature	pr_t	1.713E-08 Ωm		
(8) Coil Fill Ratio	d _{in} /d _{out}	0.49		0.2 > d _{in} /d _{out} > 0.8 is recommended for highest Q
(7) inductor inner diameter	d _{in}	3.936 mm		Inner diameter of the spiral inductor (mm or mil)
Self inductance per layer	L	0.480 μH		
Total Inductance with no target	L _{TOTAL}	1.604 μH		
(11) Sensor Operating Frequency no target	f _{RES}	8.396 MHz		
Rp with no Target	R _p	3.19 kΩ		
(9) Q factor	Q	37.00		
Self resonant frequency (estimated)	SRF	62.831 MHz		SRF should be >1.25*F _{sensor}
(12) Target Distance	D	0.800 mm		For aluminum target of at least 5 skin depths
Sensor inductance from Target Interaction	L'	0.921 μH		
(13) Sensor Frequency with Target Interaction	f _{RES'}	11.081 MHz		
Rp with Target Interaction	R _{p'}	1.68 kΩ		
(14) Q Factor with target	Q'	26.0		

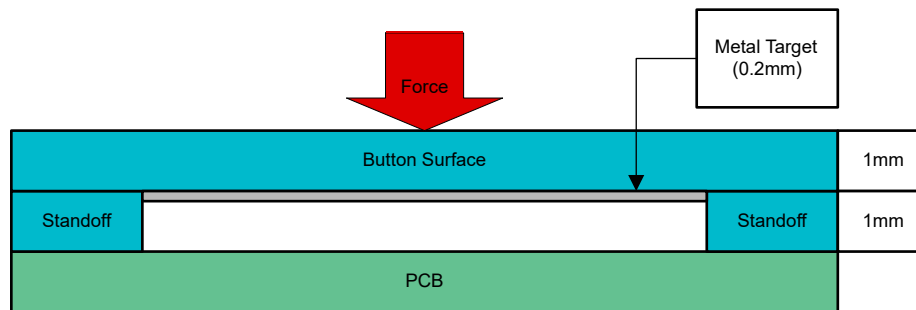
Figure 4-28. Inductive Sensing Calculator Tool - Spiral Inductor Designer tab

The results from the tool are summarized in Table 4-2.

Table 4-2. LDC Coil Calculator Outputs

Description	Designator	Value	Unit
Total Inductance with no target	L_{TOTAL}	1.604	μH
Sensor Operating Frequency no target	f_{RES}	8.396	MHz
R_P with no Target	R_P	3.19	$k\Omega$
Q factor	Q	37.00	
Self resonant frequency (estimated)	SRF	62.831	MHz
Target Distance	D	0.800	mm
Sensor Inductance from Target Interaction	L'	0.921	μH
Sensor Frequency with Target Interaction	f_{RES}'	11.081	MHz
R_P with Target Interaction	R_P'	1.68	$k\Omega$
Q Factor with target	Q'	26.0	

Since a prototype button design for this design can be 3D printed, the prototype can also include the required spacer for the button design instead of having a separate spacer material as illustrated in [Figure 4-29](#). The standoff and button surfaces are both 1mm thick to provide a surface that has some slight flexibility and to set our target height as desired. Metal tape is then placed inside the button surface between the standoffs so that button surface deflects in the desired area when a force is applied to the button surface. The thickness of the tape then puts the target at about 0.8mm away from the sensor coil.


Figure 4-29. Inductive Touch Button Stackup

The material of the button surface has an impact on how much deflection can occur to the metal target. Materials that are more stiff or that absorb the force can cause less deflection and therefore can require more force for a button press to be detected. This also comes into play when considering the thickness of the button surface. The [LDC Calculator Tool Spreadsheet](#) has a tab for determining the deflection of a material if the Young's Modulus and Poisson Ratio are known for the material. Since this design is 3D printed using nylon 12, a deflection of around $20\mu\text{m}$ is expected for a 2N force applied to the surface. This amount of deflection can be plenty for this button design since the target is so close to the sensor to begin with. See the [Inductive Touch System Design Guide for HMI Button Applications](#), application note for more information on button design.

5 Summary

Position sensors can be used to reliably implement various functions in automotive door handle designs. An AMR angle sensor or 3D Hall-effect sensor can enable door handle position detection for deployable door handles by measuring the angle of a rotating magnet. A Hall-effect switch can provide door open or closed detection by sensing the presence or absence of a magnet. Capacitive sensing can enable hand proximity detection and/or soft touch detection. Finally, soft touch and or push button detection can be implemented using inductive sensors. Design examples presented are based on a demo which is also featured in the demo video [Designing With Position Sensors: Automotive Door Handles](#) and the [Position Sensing in Automotive Door Handle Systems](#) application brief.

6 References

- [Designing with position sensors: Automotive door handles](#), video.
- Texas Instruments, [Position Sensing in Automotive Door Handle Systems](#), application brief.
- Texas Instruments, [TI Magnetic Sense Simulator \(TIMSS\)](#), simulation tool.
- Texas Instruments, [Capacitive Proximity Sensing Using the FDC1004](#), application note.
- Texas Instruments, [Inductive Sensing Overview](#), video.
- Texas Instruments, [Common Inductive and Capacitive Sensing Applications](#), application note.
- Texas Instruments, [LDC Target Design](#), application note.
- Texas Instruments, [Inductive Touch System Design Guide for HMI Button Applications](#), application note.
- Texas Instruments, [Sensor Design for Inductive Sensing Applications Using LDC](#), application note.
- Texas Instruments, [LDC Sensing Design Calculator Tool](#), simulation tool.

IMPORTANT NOTICE AND DISCLAIMER

TI PROVIDES TECHNICAL AND RELIABILITY DATA (INCLUDING DATA SHEETS), DESIGN RESOURCES (INCLUDING REFERENCE DESIGNS), APPLICATION OR OTHER DESIGN ADVICE, WEB TOOLS, SAFETY INFORMATION, AND OTHER RESOURCES "AS IS" AND WITH ALL FAULTS, AND DISCLAIMS ALL WARRANTIES, EXPRESS AND IMPLIED, INCLUDING WITHOUT LIMITATION ANY IMPLIED WARRANTIES OF MERCHANTABILITY, FITNESS FOR A PARTICULAR PURPOSE OR NON-INFRINGEMENT OF THIRD PARTY INTELLECTUAL PROPERTY RIGHTS.

These resources are intended for skilled developers designing with TI products. You are solely responsible for (1) selecting the appropriate TI products for your application, (2) designing, validating and testing your application, and (3) ensuring your application meets applicable standards, and any other safety, security, regulatory or other requirements.

These resources are subject to change without notice. TI grants you permission to use these resources only for development of an application that uses the TI products described in the resource. Other reproduction and display of these resources is prohibited. No license is granted to any other TI intellectual property right or to any third party intellectual property right. TI disclaims responsibility for, and you will fully indemnify TI and its representatives against, any claims, damages, costs, losses, and liabilities arising out of your use of these resources.

TI's products are provided subject to [TI's Terms of Sale](#) or other applicable terms available either on [ti.com](https://www.ti.com) or provided in conjunction with such TI products. TI's provision of these resources does not expand or otherwise alter TI's applicable warranties or warranty disclaimers for TI products.

TI objects to and rejects any additional or different terms you may have proposed.

Mailing Address: Texas Instruments, Post Office Box 655303, Dallas, Texas 75265
Copyright © 2024, Texas Instruments Incorporated